International Journal of Robotics and Control Systems
Vol. 4, No. 3, 2024, pp. 1403-1428
ISSN 2775-2658
http://pubs2.ascee.org/index.php/ijrcs

EEG-Based Lie Detection Using Autoencoder Deep Learning with Muse II Brain Sensing

Arya Tandy Hermawan [a,b,1], Ilham Ari Elbaith Zaeni [a,2,*], Aji Prasetya Wibawa [a,3], Gunawan [b,4], Nickolas Hartono [b,5], Yosi Kristian [b,6]

[a] Department of Electrical and Informatics, Univesitas Negeri Malang, Jawa Timur, Indonesia
[b] Department of Informatics, Institut Sains dan Teknologi Terpadu Surabaya, Jawa Timur, Indonesia
[1] arya.tandy.2205349@students.um.ac.id; [2] ilham.ari.ft@um.ac.id; [3] aji.prasetya.ft@um.ac.id; [4] gunawan@stts.edu; [5] nickolas.h20@mhs.istts.ac.id; [6] yosi@stts.edu
* Corresponding Author

ARTICLE INFO

Article history
Received June 26, 2024
Revised August 05, 2024
Accepted August 15, 2024

Keywords
Autoencoder;
Deep Learning;
Lie Detection;
Electroencephalogram;
EEG;
Muse II

ABSTRACT

Detecting deception has significant implications in fields like law enforcement and security. This research aims to develop an effective lie detection system using Electroencephalography (EEG), which measures the brain's electrical activity to capture neural patterns associated with deceptive behavior. Using the Muse II headband, we obtained EEG data across 5 channels from 34 participants aged 16-25, comprising 32 males and 2 females, with backgrounds as high school students, undergraduates, and employees. EEG data collection took place in a suitable environment, characterized by a comfortable and interference-free setting optimized for interviews. The research contribution is the creation of a lie detection dataset and the development of an autoencoder model for feature extraction and a deep neural network for classification. Data preparation involved several pre-processing steps: converting microvolts to volts, filtering with a band-pass filter (3-30Hz), STFT transformation with a 256 data window and 128 overlap, data normalization using z-score, and generating spectrograms from power density spectra below 60Hz. Feature extraction was performed using an autoencoder, followed by classification with a deep neural network. Methods included testing three autoencoder models with varying latent space sizes and two types of classifiers: three new deep neural network models, including LSTM, and six models using pre-trained ResNet50 and EfficientNetV2-S, some with attention layers. Data was split into 75% for training, 10% for validation, and 15% for testing. Results showed that the best model, using autoencoder with latent space size of 64x10x51 and classifier using the pre-trained EfficientNetV2-S, achieved 97% accuracy on the training set, 72% on the validation set, and 71% on the testing set. Testing data resulted in an F1-score of 0.73, accuracy of 0.71, precision of 0.68, and recall of 0.78. The novelty of this research includes the use of a cost-effective EEG reader with minimal electrodes, exploration of single and 3-dimensional autoencoders, and both non-pretrained classifiers (LSTM, 2D convolution, and fully connected layers) and pretrained models incorporating attention layers.

1. Introduction

Lying is a deliberate act of manipulating information, behavior, and self-representation to deceive others, protect secrets or reputations, or avoid punishment. Traditional lie detection methods, such as the polygraph, rely on physiological responses like heart rate, respiration, and skin conductivity, which can be unreliable and subject to manipulation. Advances in brain imaging technologies, specifically Electroencephalography (EEG), offer new avenues for detecting deception by directly monitoring brain activity. Despite the progress, a significant research gap exists in developing affordable, non-invasive, and reliable lie detection systems. This research aims to address this gap by leveraging EEG data analyzed with deep learning methodologies to create a more accurate and reliable lie detection system.

EEG technology has significantly improved with devices like the Muse II Brain Sensing Headband, a wireless tool that records brain activity and transmits data to connected devices. By utilizing Bluetooth technology and available open source libraries, the Muse II Headband can seamlessly transmit EEG data to smartphones or laptops, facilitating real-time analysis. This approach aims to leverage the capabilities of EEG to provide a more robust solution for lie detection.

Previous studies have explored various techniques for lie detection using EEG, but many have limitations in terms of accuracy, practicality, and cost. For instance, traditional methods require complex setups and are not easily accessible for widespread use. There is a need for a practical and effective tool that can be used in everyday settings without extensive equipment or expertise. Some studies have shown better performance but used different datasets and machine learning methods. This research contributes to the field by developing a lie detection system that is both accessible and efficient, utilizing the Muse II Headband and advanced deep learning techniques.

Data was acquired from 34 participants aged 16-25, comprising 32 males and 2 females, with backgrounds as high school students, undergraduates, and employees. EEG data collection occurred in a quiet, comfortable setting for interviews. Participants wore the Muse reader, and recording was conducted via Bluetooth-connected computers. Each participant read a provided scenario story, followed by answering 7 control questions (unrelated to the scenario) honestly and 7 relevant questions (related to the scenario) which they could answer truthfully or deceitfully, labeling their answers accordingly via keyboard input. The study was conducted with the informed consent of all participants, ensuring ethical considerations were addressed.

Data preparation involved several preprocessing steps. Initially, the EEG signals from the Muse 2 headband underwent adequate signal conditioning and hardware filtering. Subsequently, software preprocessing was applied, including converting microvolts to volts, filtering with a band-pass filter (3-30Hz), performing STFT transformation with a 256 data window and 128 overlap, normalizing data using z-score, and generating spectrograms from power density spectra below 60Hz. These steps were implemented using Python libraries such as scipy, sklearn, Matplotlib, and OpenCV. The preprocessing was designed to provide sufficient image data to accurately represent the EEG signals for detection purposes.

Feature extraction was performed using an autoencoder, followed by classification with deep neural networks. We tested three autoencoder models with varying latent space sizes and two types of classifiers: three new deep neural network models, including LSTM, and six models using pre-trained ResNet50 and EfficientNetV2-S, with some incorporating attention layers to improve performance. The autoencoder architecture used Conv2D, BatchNormalization2D, and ReLU activation in the encoder and ConvTranspose2D, BatchNormalization2D, and ReLU activation in the decoder. Training was performed over 5000 epochs using the ADAM optimizer and MSE loss. Classifier models used a combination of Conv2D, LSTM, Fully Connected layers, dropout, and the training approach (Stochastic Gradient Descent, Binary Cross Entropy loss). Pre-trained models included variations with latent operation and multi-head attention layers.

The autoencoder was chosen for its efficiency in reducing the dimensionality of complex EEG signals without losing information, its unsupervised nature, and its ability to detect anomalies

potentially related to lying. The use of pre-trained networks aimed to improve accuracy, training speed, and data efficiency, given their training on large datasets.

The system's performance was evaluated using confusion matrix metrics such as accuracy, precision, recall, and F1-score. Data was split into 75% for training, 10% for validation, and 15% for testing. The process flow diagram block is shown in Fig. 1. Efforts to minimize bias included interviewing participants about their health, mood, and stress levels, and ensuring a quiet, comfortable, well-lit environment free of distractions. Recordings were conducted after participants had sufficient rest to ensure reliable EEG data.

Key Contributions of This Research:

1. Developing an accessible and efficient lie detection system using EEG data and deep learning techniques. This system leverages the Muse II Headband for data acquisition, ensuring ease of use and affordability.
2. Exploring various deep learning architectures, including single and 3-dimensional autoencoders, and both non-pretrained classifiers (LSTM, 2D convolution, and fully connected layers) and pretrained models incorporating attention layers, to enhance the performance and reliability of the lie detection system.

Data Sufficiency and Challenges:

The initial study involved 34 participants, generating 476 data points across 5 EEG channels, resulting in 2380 data spectrograms. While this dataset was deemed sufficient during the planning phase, considering the use of pre-trained models trained on large datasets, it was recognized that increasing the number of participants and ensuring a balanced dataset of truthful and deceptive responses could further enhance the system's accuracy and robustness.

This research aims to create a practical and effective lie detection tool, contributing to the development of accessible and efficient EEG-based lie detection systems using state-of-the-art deep learning models.

2. Related Works

Lie detection has become a focal point of research across various disciplines due to the critical importance of distinguishing between truth and deception in areas such as law enforcement, psychology, and social interactions. Previous studies have extensively explored diverse approaches and methodologies in order to address the complex challenge of detecting deception, with the ultimate goal of developing reliable and accurate methods for identifying deceptive behavior.

2.1. Lie Detection Techniques

- The Brain Fingerprinting: This method uses EEG to analyze brain wave reactions to crime-related stimuli, identifying recognition of crime details by detecting unique brain wave patterns. It achieved 100% accuracy in over 120 tests involving federal agents and felony cases [1], [2]. Despite its effectiveness, its use in court remains debated due to legal admissibility concerns.
- Brain Electrical Oscillation Signature Profiling (BEOSP): Measures brain wave patterns through Power Spectral Density features to detect familiar and unfamiliar objects. Developed in the USA, BEOSP can identify if a person remembers crime details, even if suppressed, though its legal use is still under scrutiny [3].
- Speech Processing Techniques**:** Analyse speech patterns to identify lies, using SVM-based classifiers to extract meaningful features and improve accuracy, aiming to outperform traditional EEG-based methods [4].

2.2. EEG Analysis in Various Applications

- Forecasting and Prediction:

- LSTM neural networks combined with PSO models and bi-fold attention have shown superior performance in forecasting [5].
- Smoothed-CNN outperformed MLP and LSTM in predicting web guest visit data with a low MSE [6].

- Health and Concentration Detection:
  - Using ANN on Alpha and Beta frequency bands, EEG can estimate concentration levels with 73.8% accuracy [7].
  - For epilepsy detection, a combination of DWT and LBPTH achieved over 99% accuracy with SVM and KNN classifiers [8].
  - An automated deep learning framework utilizing CNN models for epileptic seizure detection bypassed manual feature extraction, demonstrating high accuracy [9].
  - EEG has also been used to detect driver drowsiness with ANN Backpropagation, achieving a MAPE of 0.02% and 90% accuracy [10].

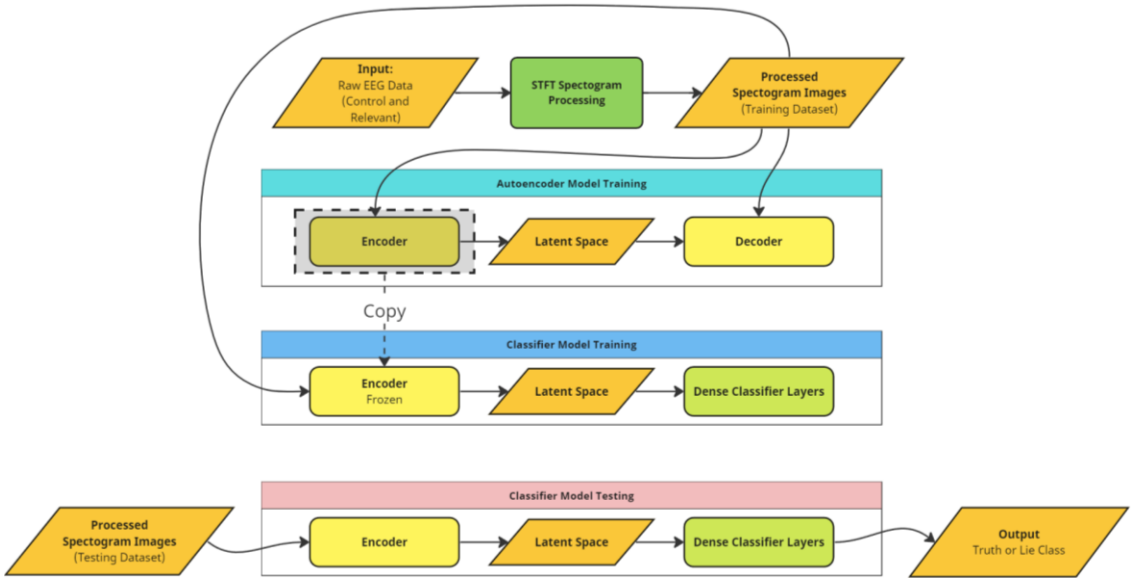

Fig. 1. Program flow diagram

2.3. EEG-Based Lie Detection

- P300 Event-Related Potential (ERP): This signal, appearing about 300 milliseconds after stimulus perception, is most sensitive in the parietal and central brain regions. Studies have effectively used P300 to detect facial familiarity in lie detection [11], [12].
- Alpha Waves and Frontal Lobe Activity: Research has shown that EEG signals, particularly alpha waves from frontal and midline electrodes, can reveal the relationship between lying and frontal lobe activity. Using neural networks and Short-time Fourier Transform (STFT), Multi-layer Perceptron (MLP) methods can distinguish between truth and deception [13].
- Support Vector Machine (SVM) Algorithm: An experiment introduced the use of the SVM algorithm to detect lies from EEG signals. The ERP method was used to preprocess the P300 wave from the EEG. The SVM algorithm then classified the preprocessed data, identifying the most probable hyperplane to separate truthful and deceptive responses [14].

2.4. Datasets and Models for Lie Detection

- Nwogu's Dataset: Created a dataset for lie detection in a natural setting where subjects were encouraged to tell high-stake lies. Respondents were given a scenario and then interrogated with casual and scenario-involved questions [15].

- CNN for Lie Detection: This research used the Dryad dataset with 12 EEG channels and their own dataset with 14 EEG channels. The ERP method was used to preprocess the P300 wave from the EEG. The model took 14-channel EEG signals as input to a convolution neural network, classifying the signal into truth or lies with up to 82% accuracy [16]. Their proposed model architecture can be seen in Fig. 2.

S.No.	Layer Type	Activation	Output Shape	Kernel-size	No. of filters	Strides	Total params
0	Input	-	14000, 1	-	-	-	-
1	Conv1D	ReLU	4667, 32	3	32	3	128
3	Conv1D	ReLU	2334, 64	3	64	2	6208
4	MaxPooling	-	1167, 64	3	-	-	0
5	Conv1D	ReLU	584, 96	3	96	2	18528
6	MaxPooling	-	292, 96	3	-	-	0
7	Conv1D	ReLU	146, 128	3	64	2	36992
8	MaxPooling	-	73, 128	3	-	-	0
16	Dropout (0.25)	-	73,128	-	-	-	0
17	Fully connected layer	ReLU	150	-	-	-	1401750
18	Dropout (0.5)	-	150	-	-	-	0
19	Classification Layer	Softmax	2	-	-	-	302

==========

Total params: 1463908, Trainable params: 1463908, Non-trainable params: 0

Fig. 2. CNN architecture used in lie detection research

2.5. Datasets and Models for Lie Detection

- To Temporal Autoencoder: Achieved high AUROC and AUPRC values for semi-supervised clustering and classification of intracranial EEG data with minimal gold standard labels [17].
- Deep Sparse Autoencoder (DSAE): Combined with CNN and LSTM for EEG emotion recognition, significantly outperforming existing models with 76.70% accuracy for valence and 81.43% for arousal on the DEAP dataset [18].
- Sequence-to-Sequence Autoencoder: In multimodal EEG analysis, this model with LSTM and CNN successfully predicted fNIRS signals from EEG data, demonstrating the predictive power of higher frequency EEG ranges [19].
- Multi-Modal Domain Adaptive Variational Autoencoder (MMDA-VAE): Improved emotion recognition with minimal calibration samples by leveraging past session data and adversarial learning, showing enhanced performance on SEED and SEED-IV datasets [20].
- Latent Factor Decoding with VAE: Enhanced cross-subject emotion recognition using multichannel EEG, proving superior to traditional methods like ICA [21].
- Deep Autoencoder-Based Feature Extraction: Achieved 97% accuracy in epilepsy detection, surpassing PCA and enabling efficient real-time monitoring with IoMT devices [22]. A shallow autoencoder framework combined with kNN and SVM classifiers demonstrated high-performance seizure detection with single-channel EEG, reaching up to 99.19% accuracy. These studies highlight the versatility and efficacy of autoencoders in advancing EEG analysis for various applications [23].

3. Proposed Work

In this research, deep learning technique that involves autoencoder model and deep neural network model will be used. The autoencoder model acts as a feature extractor for EEG data in form of spectrograms [24], [25] and the deep neural network model acts as a classifier to determine whether the response is truth or lie. After the model is trained, its effectiveness evaluated using a separate

testing set consisting of 28 data samples. The acquired results will undergo further analysis to assess the model's performance and gain valuable insights from the evaluation process. Fig. 3 shows the proposed work flowchart.

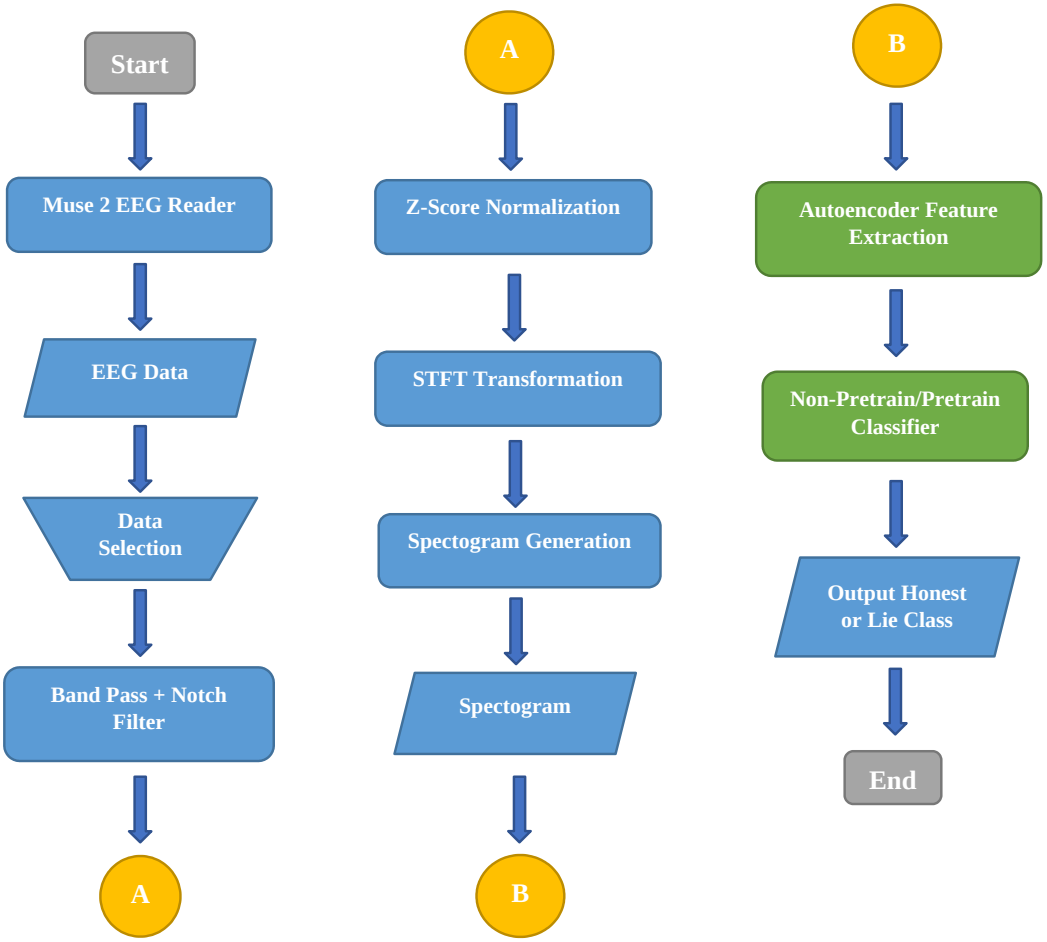

Fig. 3. Proposed Work Flowchart

3.1. Dataset

We created a dataset for lie detection that closely resembles real-life scenarios. In this dataset, individuals are presented with a problem and asked questions related to the problem. Additionally, they are given control questions that are unrelated to the discussed issue, serving as a baseline, and relevant questions specifically related to the discussed problem, similar to existing deception detection techniques. The dataset aims to simulate a realistic environment and provide a comprehensive set of questions to evaluate deception detection methods effectively [15], [26].

Data was acquired from 34 participants aged 16-25 (32 males and 2 females), including high school students, undergraduates, and educated employees. Participants were instructed to be well-rested and avoid substances affecting brain activity. To ensure data quality, participants were instructed to be well-rested and avoid substances affecting brain activity. They were briefed on remaining still, avoiding unnecessary movements, and keeping their eyes closed to minimize EEG artifacts. Data collection occurred in a quiet, comfortable, well-lit room to ensure accurate recording. Participants were seated comfortably to maintain a calm atmosphere and reduce potential noise and artifacts.

The collection of EEG data involving human participants necessitates stringent ethical considerations. This study was conducted in a university laboratory, following procedures approved and supervised by the head of the laboratory to ensure ethical and safety standards. Participants were thoroughly informed about the study's nature and purpose, and their consent was obtained. The study

adhered to ethical guidelines to protect participants' rights and well-being. Although formal Institutional Review Board (IRB) [27] approval was not used, the experimental procedures were closely monitored to maintain ethical standards. All data collected was anonymized to ensure participant confidentiality.

The dataset utilized in this research is a raw EEG dataset comprising five channels: TP9, Fp1, Fp2, TP10, and FPZ. Data collection was performed using the Muse II Headband, an EEG device equipped with five electrodes that generate recordings across these five channels. A custom-made dataset collector application was employed to connect the Muse II Headband to a laptop via Bluetooth, facilitating the storage of brainwave signals in CSV format.

The data collection process began with providing respondents with detailed instructions, such as keeping their eyes closed during recording and avoiding blinking. After these instructions were clearly communicated, respondents participated in a scenario reading session. During this session, they were presented with randomly assigned scenarios, which could be either positive or negative. Respondents were then given 5-10 minutes to read and comprehend the scenarios.

After completing the scenario reading, respondents were fitted with the Muse II Headband and instructed on its proper use. They were asked to wear the headband on their forehead and undergo a calibration process. During calibration, respondents blinked repeatedly. If spikes appeared in both the TP9 and TP10 channels simultaneously with the blinking, it confirmed that the Muse II Headband was correctly positioned, and the calibration process was considered complete. Following successful calibration, the interrogation and recording session commenced.

During the interrogation and data recording session, respondents were asked to close their eyes and answer 14 questions (7 pairs of questions) provided to them. Each pair began with a control question followed by a relevant question. The recording lasted for 10 seconds per question, starting when the question was read aloud. Respondents were expected to give concise, clear, and brief answers within this time frame. To minimize noise interference in the recorded data, they were instructed not to blink during the recording process. After each question's recording session, respondents labeled the recorded data, which was crucial for obtaining ground truth information for each recording. Fig. 4 shows the process of acquiring and recording EEG data with participants.

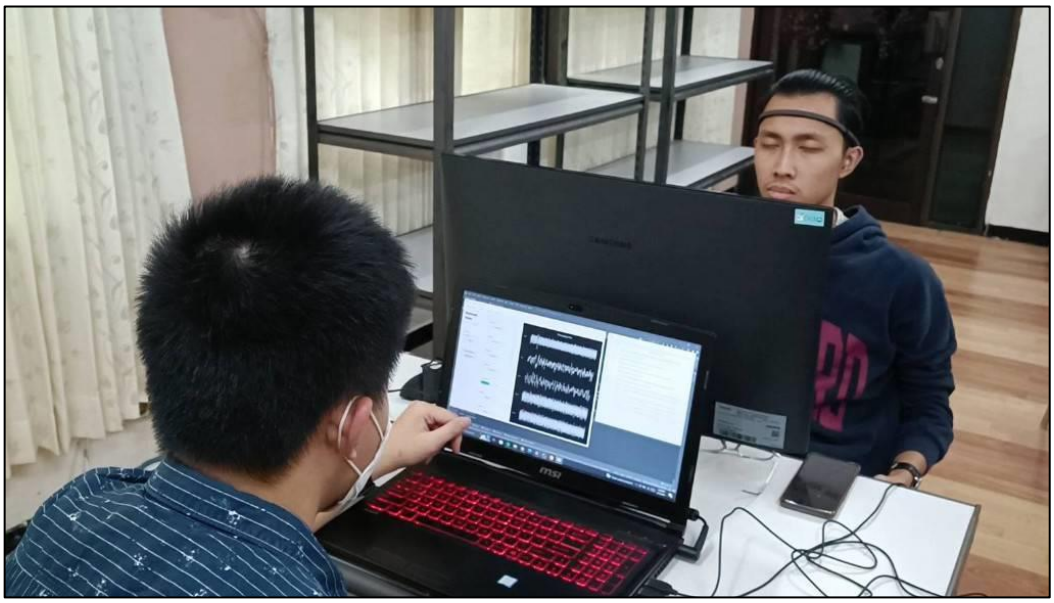

Fig. 4. Data aquizition and recording session

We acknowledge the potential for human error in the calibration process and manual labeling of data by respondents. Due to the need for interaction with participants, automated labeling is not feasible. To mitigate errors, we implemented a structured calibration process with blinking exercises to ensure correct placement of the Muse headband, repeating until reliable signals were obtained.

Participants received detailed instructions and training for accurate labeling, with supervision by trained researchers to verify correctness in real-time. These measures enhance the reliability and validity of the ground truth data used for training and validation.

Each CSV file represents the recording of a question along with the respondent's answer, spanning a duration of 10 seconds. Each file contains 2560 rows and 8 columns. The number of rows corresponds to the sampling frequency of the Muse II Headband, which is 256 Hz, meaning the device produces 256 data samples per second. The columns in the file represent the collected data for each sample and include the following: ID, TP9, Fp1, Fp2, TP10, Fpz, marker, and timestamp. For further processing, only the data in columns 2 to 6, corresponding to each EEG channel, will be utilized.

The total number of data points obtained from the recording process is 476, consisting of 238 control data points and 238 relevant data points. However, some data will be discarded due to various issues, such as improper device placement resulting in imperfect recordings or errors in labeling the control data. Specifically, 22 pairs of data will be excluded due to significant artifacts such as large muscle movements, eye blinks during recording, or device misplacements. This exclusion ensures that flawed data do not interfere with the training process of the model. The detailed distribution of the EEG dataset is shown in Table 1.

Table 1. Distribution of honest and lie data

N	Type	Amount (In Pairs)
1	Honest	112 Pairs
2	Lie	104 Pairs

3.2. STFT-Spectrogram Processing

In this study, we propose to use the Short-Time Fourier Transform (STFT) to decompose EEG signals from the time domain into the frequency domain [28]. The resulting decomposition will be represented as spectrogram images, which will serve as input for training the neural network mode. STFT was chosen due to its ability to provide a time-frequency representation, which is crucial for analyzing non-stationary signals like EEG. Unlike Wavelet Transform or Short-Time Energy, STFT offers a balanced resolution in both time and frequency domains, making it suitable for capturing the dynamic nature of EEG signals. Although wavelets can analyze signals at various scales and might be computationally complex, they offer significant advantages for future research considerations. To remove raw signal noise from EEG data acquired during the recording process, a filtering process is employed. This involves using low-pass and high-pass filters to isolate the EEG frequency band, and a notch filter to eliminate power line noise [29]. Spectrogram generation is a crucial step, as it ensures that machine learning algorithms can effectively learn from the input data and produce accurate results. Proper spectrogram processing can also enhance the performance of the machine learning algorithms used.

A. Data Pairing, Feature Selection, and Conversion

At this stage, the recorded data will be grouped according to their paired questions. This grouping is necessary because the model requires input in the form of two files: one for the control question recording and one for the relevant question recording. Once the data is grouped into pairs, each pair will be labeled based on the labels of the relevant question recordings. The data used in the training process are found in columns 2 to 6 of the CSV file. These columns contain the EEG recordings for each channel in microvolts (μV). The remaining columns are irrelevant and will not be used in the training process. When processing raw EEG data, it is typically handled in volts (V). Therefore, the existing data in microvolts (μV) must be converted. After conversion, the data will undergo a filtering process to remove noise and irrelevant frequencies, preparing it for the subsequent training process.

B. Filtering

Filtering is a signal processing technique used to remove unwanted frequency components from a signal. In recorded EEG (Electroencephalography) data, obtained from headband sensors, filtering

cleans the raw signal by eliminating noise and artifacts that can obscure true neural activity. This process involves applying mathematical functions to the EEG data to selectively attenuate or amplify specific frequency bands, resulting in a clearer and more interpretable signal.

In EEG preprocessing, filtering serves several key functions [30]-[32]. Firstly, it reduces noise from various sources, such as environmental interference, electrical equipment, and physiological artifacts like eye movements and muscle activity. Secondly, it enables the extraction of relevant frequency bands associated with different brain activities, such as delta, theta, alpha, beta, and gamma waves. By focusing on these specific bands, researchers can better analyze and interpret the underlying neural processes. Overall, filtering enhances the signal-to-noise ratio, making subsequent analysis more accurate and meaningful.

In this paper, band-pass filters with cutoff frequencies oh 8Hz and 30 Hz will be utilized to selectively remove signals outside a specified frequency range. This type of filter is commonly used in signal processing to isolate specific components within a signal, thus facilitating the analysis process. Band-pass filters will be applied to eliminate irrelevant frequencies in the recorded EEG data. This is necessary because the human brain produces specific EEG waves with frequencies up to 100 Hz [33]. Notch filters with a center frequency of 50 Hz will be used to eliminate power line noise. The band-pass Butterworth filter is represented by Equation (1).

$$H(s) = \frac{\omega_H s^2}{(s^2 + \omega_L s + \omega_L^2)(s^2 + \omega_H s + \omega_H^2} \tag{1}$$

s is a complex frequency variable

$$\text{where} \quad \omega_{low} = 2\pi \frac{f_{low}}{f_s} \quad \text{and} \quad \omega_{high} = 2\pi \frac{f_{high}}{f_s} \tag{2}$$

Equation (3) shows Bilinear transformation is used for conversion to discrete domain:

$$s = \frac{2}{T} \frac{1 - z^{-1}}{1 + z^{-1}} \tag{3}$$

In addition to band pass filters, notch filters are essential for removing specific narrow frequency bands of interference, such as power line noise at 50 Hz or 60 Hz, ensuring cleaner and more accurate signal processing in applications like EEG. Using bilinear transformation, the notch filter is formulated as in equation (4).

$$H(s) = \frac{s^2 + \omega_{notch}^2}{s^2 + \frac{\omega_{notch}}{Q} s + \omega_{notch}^2} \tag{4}$$

Q is the quality factor of the filter

EEG signals are divided into several frequency bands, each reflecting different brain activities. Delta waves (0.5-4 Hz) appear during deep sleep and are linked to healing and regeneration. Theta waves (4-8 Hz) are associated with light relaxation, meditation, and REM sleep. Alpha waves (8-13 Hz) dominate when a person is calm and relaxed, often with closed eyes but awake. Beta waves (13-30 Hz) occur during active mental tasks, problem-solving, and high concentration. Gamma waves (>30 Hz) are related to high-level cognitive functions like complex information processing and sensory integration. Each frequency band provides unique insights into various brain states and functions.

In our research on lie detection, the most influential brain waves are theta, alpha, and beta waves, which fall within the 3 Hz to 30 Hz range. Frequencies outside this range are discarded to prevent noise and improve the performance of the machine learning algorithm. After filtering, the data undergoes a transformation process to alter its representation format for further analysis.

We ensured the data collection environment was as noise-free as possible and implemented protocols to minimize artifacts from muscle movements, especially around the eyes. Additionally, evaluations conducted in our lab using EEG signal reading and visualization applications indicated that the signals from the Muse headband were relatively clean and free from noise. We applied band-pass filtering to further refine the data. Furthermore, by using spectrograms, we truncated the frequency spectrum above 60Hz to ensure only beta, alpha, and theta signals were used. The normalization process also helps to automatically eliminate the influence of artifacts, which typically have large amplitudes, ensuring cleaner and more reliable EEG data for analysis.

C. Transformation

The transformation of signals from the time domain to the frequency domain involves converting a time-based signal, which represents how a signal varies over time, into its frequency components, which represent how much of the signal lies within each given frequency band over a range of frequencies.

The purpose of applying the Short-Time Fourier Transform (STFT) to EEG signals is to analyze the signal's frequency content over time. EEG signals are inherently non-stationary, meaning their frequency components change over time. The STFT achieves this by dividing the signal into short, overlapping time segments and performing the Fourier Transform on each segment. This results in a time-frequency representation that captures how the signal's spectral content evolves. This method is also applied in some research [34], [35] for processing EEG data. Fig. 5 shows the EEG signal representation in the time domain and frequency domain.

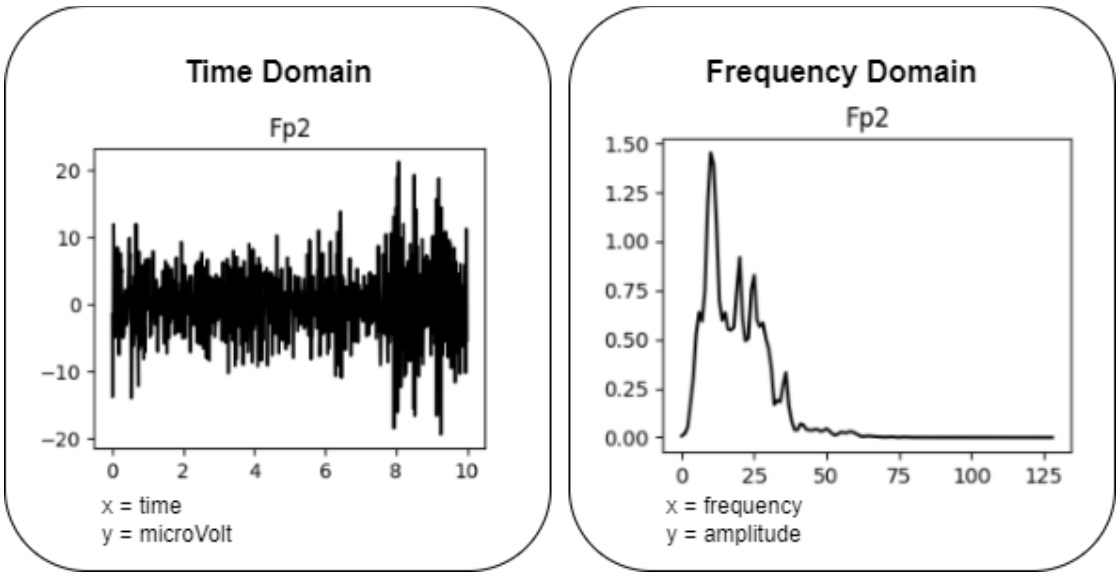

Fig. 5. Comparison of EEG data in time domain and frequency domain

The formula used for the STFT transformation of signal *x(t)* is given by equation (5) [36].

$$X(t,f) = \int_{-\infty}^{\infty} x(\tau)\omega(\tau - t)e^{-j2\pi f\tau}\, d\tau \tag{5}$$

For a discrete-time signal x[n], the STFT can be written as:

$$X[m,k] = \sum_{n=0}^{N-1} x[n]\omega[n - mR]e^{-j2\pi kn/N} \tag{6}$$

Where:

- $x[n]$ is the discrete signal
- $\omega[n\text{-}mR]$ is window function applied at time mR, R is hop size

- N is the length of the FFT applied to each windowed segment.
- k is the frequency bin index

The results of the EEG signal transformation will be used to produce a spectrogram image, which will serve as input features for deep learning in the classification of lie status. This conversion is necessary to create a spectrogram, which requires a frequency domain representation typically measured by power spectral density. The resulting power spectral density data will be further processed and normalized before generating the spectrogram. The STFT used in this research will have the following settings:

- 256 Hz sampling frequency (f_s)
- Applying a Hanning Window STFT
- 256 data points in each segment (N)
- 128 data points overlapping between segments (R)

D. Normalization

Normalization is a data preprocessing technique used to standardize input data into a more consistent format that machine learning algorithms can more easily understand. The primary goal of normalization is to ensure that the input data has a uniform scale. This is especially crucial in processing EEG data because each person's brainwave scale may vary. By normalizing the data, we equalize these scales and prevent significant differences in EEG values, ensuring a more accurate and reliable analysis. Normalization was applied per EEG channel to ensure that each feature has the same scale. This technique standardizes the data to have a mean of zero and a standard deviation of one, which simplifies the removal of artifacts and enhances the model's training performance and interpretability.

In this research, we use the Z-score normalization technique. Z-score normalization is commonly applied in EEG data processing as it standardizes the data to have a mean of zero and a standard deviation of one [37]. This normalization simplifies the removal of artifacts, making it more effective than using statistical methods like thresholding and regression. Formula 2 represents the Z-score normalization formula, where x is the data point, μ is the mean, and σ is the standard deviation.

$$z = ((x - \mu)) / \sigma \quad (7)$$

Z-score normalization will be applied to all the data within the dataset, ensuring that each feature has the same scale. This technique is particularly beneficial for machine learning algorithms, as it standardizes the input data, improving performance and expediting convergence. By ensuring a uniform scale, Z-score normalization helps the algorithms process the data more efficiently and effectively. We considered alternative normalization techniques but found them less effective for our data:

- Min-Max Normalization: Poorly handles outliers, distorting EEG signal representation.
- Robust Scaler: Less sensitive to outliers but may not standardize data effectively for deep learning.
- Log Transformation: Only works with positive values and is problematic for EEG data with both positive and negative values.

Given these limitations, Z-score normalization was chosen for its consistency and suitability for EEG signals, supporting the reliability and effectiveness of our models.

E. Spectrogram Building

The final step in the data preprocessing phase is the creation of spectrograms. Spectrograms will be generated for each available channel using the data that has undergone the previous preprocessing steps. This is a crucial step in the research, as it takes a different approach by utilizing spectrograms

of the EEG data as input for the prepared autoencoder model, instead of using raw EEG data in numerical form.

The spectrogram is depicted using the magnitude values from the following STFT transformation from the previous stage using the following equation (8) where $\Re$ is the real part and $\Im$ is the imaginary components:

$$|X[m,k]| = \sqrt{\Re(X[m,k])^2 + \Im(X[m,k])^2} \quad (8)$$

The creation of spectrograms will involve utilizing the Python library Matplotlib. A grayscale colormap setting will be used to minimize the dimensionality of the spectrograms processed by the model. Fig. 6 shows an example of the spectrograms produced by this process.

Fig. 6. Spectrogram example

In our current study, we used the Short-Time Fourier Transform (STFT) to generate spectrograms for feature extraction. This method effectively captures the frequency variations of EEG signals, which have a relatively narrow frequency range, using 50% overlapping windows.

For future research, we plan to explore additional feature extraction methods, such as wavelet [38]-[40] transform with scalograms, which provide a detailed frequency spectrum at various scales. This will allow us to capture a broader range of EEG signal characteristics, enhancing data analysis and potentially improving model performance.

3.3. Model Architecture

The model architecture combines an autoencoder model and a deep neural network (DNN) classifier model with a pre-trained model backbone. This fusion of the autoencoder and DNN model with a pre-trained model backbone allows for both unsupervised feature learning and fine-tuned classification.

A. Autoencoder

The first model is the autoencoder. It is a Deep Convolutional Neural Network that performs feature extraction on input data in the form of spectrograms. The model consists of two main parts: the encoder and the decoder. The encoder is responsible for encoding the input data into a latent space, while the decoder decodes the latent space generated by the encoder back to the original input data format [21]. In the main program, only the encoder part is used because the desired output from the autoencoder model is only the latent space of the EEG spectrogram.

During training, the decoder is used to evaluate the quality of the encoding by reconstructing the latent space back into the original input data. The more accurately the decoder can recover the original data, the better the encoder's performance in capturing important features.

Autoencoders consist of two main parts: the encoder and the decoder [41], [42]. The encoder maps the input data x to a latent space representation z, and the decoder maps z back to the reconstructed input $\hat{x}$

- Encoder:

$$z = f_\theta(x) = \sigma(W_e x + b_e) \quad (9)$$

- Decoder:

$$x^{\wedge} = g_{\Phi}(z) = \sigma(W_d z + b_d) \quad (10)$$

Where:

- W_e and b_e are the weights and biases of the encoder
- W_d and b_d are the weights and biases of the decoder
- σ is an activation function (ReLU or sigmoid)

The autoencoder architecture utilizes a combination of Conv2D, BatchNorm2D, and ReLU layers. The Conv2D layers use kernel sizes of 3x3 with a stride of 2x2 and padding of 1x1, allowing for detailed feature extraction. BatchNorm2D layers are applied to normalize the activations, improving the training stability and convergence. ReLU activation functions introduce non-linearity, enabling the model to learn complex patterns. The detailed architectures of the encoder and decoder are presented in Table 2 and Table 3, respectively.

Table 2. Encoder architecture

Layer	In Channels	Out Channels	Kernel	Stride	Padding
Conv2D	2	8	3x3	2x2	1x1
BatchNorm2D	8	8	-	-	-
ReLU	-	-	-	-	-
Conv2D	8	16	3x3	2x2	1x1
BatchNorm2D	16	16	-	-	-
ReLU	-	-	-	-	-
Conv2D	16	32	3x3	2x2	-
ReLU	-	-	-	-	-
Conv2D	32	64	3x3	1x1	-
ReLU	-	-	-	-	-
BatchNorm2D	64	64	-	-	-
Conv2D	64	64	3x3	2x2	1x1
ReLU	-	-	-	-	-

Table 3. Decoder architecture

Layer	In Channels	Out Channels	Kernel	Stride	Padding	Output Padding
ConvTranspose2D	64	64	3x3	2x2	1x1	1x1
BatchNorm2D	64	64	-	-	-	-
ReLU	-	-	-	-	-	-
ConvTranspose2D	64	32	3x3	1x1	-	-
ReLU	-	-	-	-	-	-
ConvTranspose2D	32	16	3x3	2x2	-	-
ReLU	-	-	-	-	-	-
BatchNorm2D	16	16	-	-	-	-
ConvTranspose2D	16	8	3x3	2x2	1x1	1x1
BatchNorm2D	8	8	-	-	-	-
ReLU	-	-	-	-	-	-
ConvTranspose2D	8	2	3x3	2x2	1x1	1x1

The latent space generated by the autoencoder has three dimensions, with a size of 64x10x51. This size was determined through experimentation to balance the complexity and representational capacity of the model. Additionally, previous studies have shown the effectiveness of using 3-dimensional latent spaces in autoencoder models. The chosen dimensions provide a compact yet informative representation of the input data, enabling the classifier model to effectively process the latent space. This resulting latent space is relatively small, making it lightweight for processing. Despite its compact size, it retains important features, enabling the classifier model to effectively process the latent space.

B. Classifier

The second model in this research is a classifier model. It is designed to classify lies or truths based on input EEG brainwave data. The classifier model utilizes a pre-trained model as its backbone. The chosen pre-trained model is EfficientNetV2-S based on [43]-[45], and [46]. EfficientNetV2-S was chosen as the backbone for classification due to its efficient architecture, which balances model complexity and performance. Its depthwise separable convolutions and compound scaling method enable it to achieve high accuracy with fewer parameters, making it suitable for handling the detailed features extracted from EEG spectrograms. The input layer and the classifier layer at the end of EfficientNetV2-S are modified to suit the task requirements. The input data, which is in the form of a latent space, is first concatenated before being processed by fine-tuned EfficientNetV2-S. The initial input layer that expects 3-dimensional input is transformed into 128 dimensions to match the latent space input. The output layer, which initially produces 1000 features, is modified to output only 1 feature to accommodate the binary classification task.

During the training process, the features in the backbone model, namely EfficientNetV2-S, will also undergo freezing or unfreezing. Initially, most layers are frozen to preserve the pre-trained weights, allowing only the top layers to be fine-tuned. As training progresses, some of the earlier layers are gradually unfrozen to adapt the entire model to the specific task of lie detection. This strategy helps retain the learned features while adapting to new data, improving the model's performance. The purpose of freezing or unfreezing layers in the pre-trained models is to avoid the need for retraining the entire model as it already has sufficiently optimized weights. Thus, it is only necessary to train a few specific layers to adapt to the required task. The EfficientNetV2-S architecture is shown in Table 4.

Table 4. EfficientnetV2-S architecture

Stage	Operator	Resolution	#Layers	Output Channel	Expansion Ratio	SE ratio
1	Conv3x3	224x224	1	24	-	-
2	Fused_MBConv1,3x3	112x112	2	24	1	-
3	Fused_MBConv4,3x3	112x112	4	48	4	-
4	Fused_MBConv4,3x3	56x56	4	64	4	-
5	MBConv4,3x3	28x28	6	128	4	0.25
6	MBConv6,3x3	14x14	9	160	6	0.25
7	MBConv6,3x3	14x14	15	256	6	0.25
Final	Conv1x1 &Pooling	7x7	1	1280	-	-
Final	FCLayer	1x1	1	1000	-	-

To mitigate potential biases introduced by using pre-trained models like EfficientNetV2-S, we tailored the input to match EEG spectrogram images and adjusted the output for binary classification. We employed a freeze-unfreeze strategy, preserving the optimal pre-trained weights by freezing most layers and training only a few specific layers relevant to our task [47]-[49]. Additionally, we compared the performance of six pre-trained models with three non-pretrained models to evaluate their effectiveness and biases, ensuring a comprehensive assessment and balanced approach to leveraging the strengths of pre-trained models while minimizing potential biases.

3.4. Performance Measurement

To assess the performance of the trained models, a validation set will be utilized. In the case of the autoencoder model, a set of 64 data samples will be reserved specifically for validation purposes. These samples will serve as a means to evaluate the quality and effectiveness of the autoencoder's reconstruction capabilities. On the other hand, for the classifier model, a validation set consisting of 14 pairs of data samples will be employed. This validation set is carefully curated to ensure an equal distribution of honest and lie data pairs. By employing an equal division, the classifier model's performance can be objectively evaluated in terms of its precision, recall, and overall accuracy.

To quantitatively measure the performance of the classifier model on the validation set, four evaluation metrics will be utilized: F1-Score, Accuracy, Precision and Recall. Precision measures the proportion of true positive predictions among all positive predictions, while Recall measures the

proportion of true positive predictions among all actual positive instances. By considering these metrics, a comprehensive evaluation of the classifier model's performance can be obtained, allowing for a reliable assessment of its effectiveness in distinguishing between honest and lie data samples. The F1-Score is a combined measure of precision and recall, providing an overall assessment of the model's ability to correctly identify both honest and lie instances. Additionally, the Accuracy metric will provide an estimation of the overall correct classification rate achieved by the classifier model on the validation set. By considering both metrics, a comprehensive evaluation of the classifier model's performance can be obtained, allowing for a reliable assessment of its effectiveness in distinguishing between honest and lie data samples.

While we recognize that this may not be entirely sufficient, it served as a preliminary evaluation. With the relatively small sample size, we also have attempted to use cross-validation techniques, and the results were similar to our reported findings. Despite the limited sample size, the best pre-trained model demonstrated a significant level of accuracy at 71%. We ensured that the testing data was distinct from the training data to maintain the integrity of our results. Cross-validation techniques were employed to validate the robustness of the models. Despite the limited sample size, the best pre-trained model demonstrated a significant level of accuracy at 71%. This underscores the potential for even better performance with an expanded dataset in future research. For future work, we plan to test the models on external datasets to further validate their robustness and generalizability. This initial success underscores the feasibility of our approach and sets the stage for more comprehensive studies with larger and more diverse datasets

To ensure the interpretability of our deep learning models, we conducted thorough evaluations of both the autoencoder feature extractors and the classifiers. Performance metrics for each model were analyzed using confusion matrices, which are detailed in the results section. Additionally, we examined the EEG signals to determine the contributions of different channels. The Fp1 and Fp2 channels were found to be the most significant. The dominant frequency bands observed were beta, alpha, and theta, which align with the participants' calm state during the trials. This detailed analysis helps provide insights into the model's decision-making process and enhances the transparency of our approach.

4. Results and Discussion

This research conducted experiments on two main aspects: the autoencoder model and the classifier model. In order to evaluate the performance of these models, dedicated test sets have been prepared for each. The test set for the autoencoder model consists of 112 data samples. This set will be used to assess the autoencoder's ability to accurately reconstruct and represent the input data, providing insights into the effectiveness of the encoding and decoding processes.

While we recognize that a larger sample size would provide a more comprehensive validation of the autoencoder model's performance, our current study with 112 data samples has yielded promising results. The autoencoder demonstrated excellent performance with a very low MSE of 0.00018, as shown in Table 5, and visual inspection of the recovery output, as shown in Fig. 7, shows high-quality reconstruction. These findings support the efficacy of our proposed model, but we plan to use a larger dataset in future research to enhance the robustness and generalizability of our results.

Table 5. Testing results of each autoencoder model comparison

No	Model Description	Test Loss
1	Proposed Model	0.00018
2	Model with 1D Latent Space	0.00845
3	Model with 3D Latent Space (32x10x51)	0.00021

For the classifier model, a separate test set comprising 28 data pair samples has been created. To ensure a fair evaluation, the data pairs are evenly distributed between honest and lie instances. This balanced distribution allows for a comprehensive assessment of the classifier's capability to correctly classify and discriminate between honest and lie data.

4.1. Autoencoder Model Experiment Results

In the autoencoder experiments, the autoencoder model proposed in this research will be compared to two other autoencoder models previously developed. The first model employs a 1-dimensional latent space with a size of 4080, while the second model incorporates a 3-dimensional latent space with dimensions of 32x10x51. These models serve as benchmarks to evaluate the performance and effectiveness of the proposed autoencoder model.

The selection of benchmark models for comparison in this study is grounded in their demonstrated success in related research areas. Previous studies have shown that autoencoder-based models are effective in various EEG applications, including emotion recognition, epilepsy detection, and cognitive state recognition. For instance, Li et al. (2020) demonstrated the effectiveness of autoencoder models in emotion recognition by comparing traditional autoencoder (AE), variational autoencoder (VAE), and restricted Boltzmann machine (RBM), showing that autoencoder-based models could effectively capture and decode latent factors. Similarly, "An Improved Approach for EEG Signal Classification using Autoencoder" used ICA and autoencoder methods to achieve 82.21% accuracy in classifying familiar and unfamiliar faces, which differs in context and methodology from our approach but serves as a benchmark for performance comparison.

Here are some comparative analyses with related studies.

- An Improved Approach for EEG Signal Classification using Autoencoder This study aimed to enhance the classification of familiar and unfamiliar faces using EEG signals through a novel deep learning-based approach for deception detection [50]. By implementing an autoencoder to classify EEG signals processed through Independent Component Analysis (ICA), the study significantly improved upon traditional machine learning methods. The proposed model achieved a state-of-the-art mean accuracy of 82.21%, demonstrating its effectiveness and superior performance in classifying familiar and unfamiliar EEG signals compared to conventional techniques. In our study, we utilized a different preprocessing method (STFT) and focused on lie detection, showing that while both studies use autoencoders, the context and application differ.
- Improved semi-supervised autoencoder for deception detection This study aimed to improve speech-based deception detection with a semi-supervised additive noise autoencoder (SS-ANE) model that used both labeled and unlabeled data [51]. Technically, the SS-ANE model incorporated specific activation functions and dropout layers to prevent overfitting, enhancing the traditional autoencoder. The novelty was its application to deception detection. Contributions included creating a Chinese deception speech corpus and demonstrating the model's effectiveness. The model achieved 62.78% accuracy on the CSC corpus with 1000 labeled examples and 63.89% on the Chinese corpus with 200 labeled examples, outperforming existing methods. Our approach differs by focusing on EEG data and using a fully supervised learning technique, highlighting the variability in results due to different data types and methodologies.
- LieWaves: dataset for lie detection based on EEG signals and wavelets This study aimed to create an EEG-based dataset for lie detection, utilizing the Emotiv Insight device to collect EEG signals from 27 individuals during honest and deceitful trials [52]. The data underwent preprocessing with the ATAR algorithm for artifact removal and the OSW method for augmentation, followed by feature extraction using DWT and FFT. Classification was performed with CNN, LSTM, and CNN-LSTM models. The novelty was the introduction of the LieWaves dataset, addressing gaps in EEG-based lie detection research. The study achieved a high accuracy of 99.88% with the LSTM and DWT techniques, demonstrating the dataset's effectiveness. In contrast, our research used the Muse II device and focused on STFT for preprocessing, aiming to validate the effectiveness of our approach in a different experimental setup.
- Comprehensive Review of Lie Detection in Subject Based Deceit Identification This study aimed to improve deception detection using EEG data by distinguishing between innocent and culpable individuals [53]. The main contribution was employing a deep learning method that combined Restricted Boltzmann Machines (RBMs) with wavelet transforms to extract time and frequency

domain features. The novelty was in using a deep belief network (DBN) composed of four stacked RBMs with softmax regression, a method rarely applied in this field. Methodology included preprocessing EEG data to utilize smaller fragments, creating temporal feature maps to enhance classifier performance. The study demonstrated improved accuracy using CIT-based EEG data, validating the proposed techniques for effective deception analysis. Our research builds on this by employing autoencoders and pre-trained networks for feature extraction and classification, offering a different perspective on handling EEG data for lie detection.

In our research, we compared one-dimensional and three-dimensional autoencoder models to validate the effectiveness of using latent spaces in autoencoders. The three-dimensional latent space model (32x10x51) initially showed superior performance. To enhance this further, we increased the first dimension, resulting in a latent space of 64x10x51. This selection aims to demonstrate the superior performance of three-dimensional latent spaces in autoencoder models, thereby supporting the efficacy of our approach in EEG-based lie detection.

In our study, we conducted a thorough analysis that included data collection, data splitting, model training, and both qualitative and quantitative evaluations. Quantitative analysis was performed using Mean Squared Error (MSE) loss to achieve the smallest loss, ensuring the spectrogram information captured in the latent space is accurately represented for the classifier input. Qualitative analysis involved visually inspecting the reconstruction results of the autoencoder to select the best model.

We experimented with several methods and reported those with the best performance based on previous research and our findings. This combined approach ensured a robust evaluation of our autoencoder models, effectively demonstrating their ability to capture essential features of the input data. During the training process, the Adam (Adaptive Momentum) optimizer will be utilized along with the Mean-Squared Error (MSE) loss function. The Adam optimizer provides efficient gradient-based optimization, helping to enhance the convergence and stability of the training process. The MSE loss function, commonly used for autoencoder models, measures the discrepancy between the reconstructed output and the original input data. To control the learning process, a learning rate of 1e-4 has been employed.

After conducting tests on the testing set, we evaluated the performance of all three autoencoder models. The comprehensive results have been tabulated in Table 5, providing a clear overview of their respective outcomes. This table shows the loss of all three autoencoder models on the testing set. Statistical significance tests were conducted to validate the differences in MSE losses between the proposed and benchmark autoencoder models. The results indicated that the proposed model significantly outperformed the benchmarks. Observed trends in spectrogram reconstructions showed that the proposed model consistently produced higher quality reconstructions, particularly in retaining fine details in the spectrograms. Fig. 7, Fig. 8, and Fig. 9 illustrate the spectrogram input data and the corresponding recovered spectrogram input by the three autoencoder models. In those figures, we can observe top-bottom comparisons of the original input data and the reconstructed output produced by each model. In the top section of each figure, the original input data is presented, providing a clear representation of the initial data points. In the bottom section, the corresponding recovered input produced by each model is showcased, allowing for a direct evaluation of the model's ability to reconstruct the input accurately. This visual representation enables us to assess the models' ability to capture and reproduce the essential features of the input data accurately.

For this study, we used Mean Squared Error (MSE) to evaluate the performance of our autoencoder model. MSE was chosen to ensure that the spectrogram information captured in the latent space is accurately represented for the classifier input. However, we recognize the value of additional metrics such as Peak Signal-to-Noise Ratio (PSNR) and Structural Similarity Index (SSI), which are commonly used for assessing the quality of compressed or regenerated images [54]-[56]. In future research, we will incorporate PSNR and SSI [57] alongside MSE to provide a more comprehensive evaluation of the autoencoder's performance. This will ensure a more thorough assessment of the model's capabilities in accurately capturing and regenerating spectrogram information.

International Journal of Robotics and Control Systems
Vol. 4, No. 3, 2024, pp. 1403-1428
ISSN 2775-2658

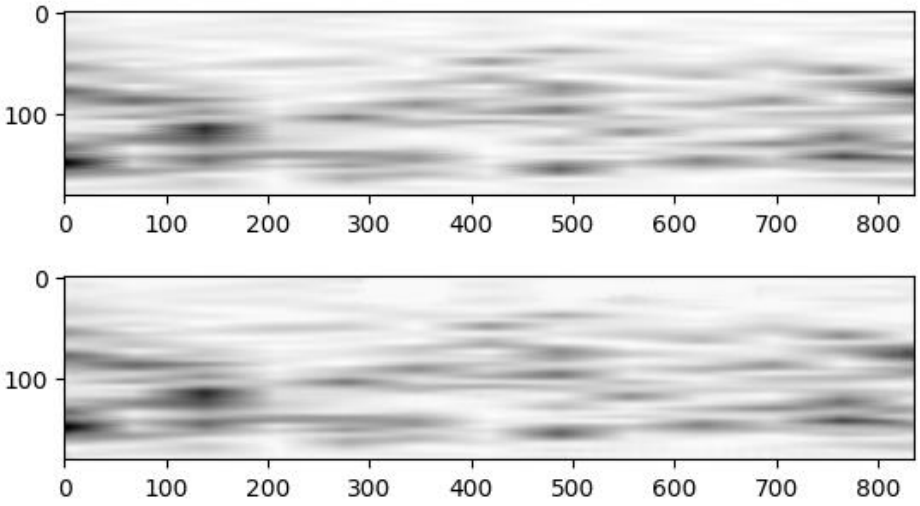

Fig. 7. Comparisons of spectrogram input data and recovered spectrogram input of the proposed model

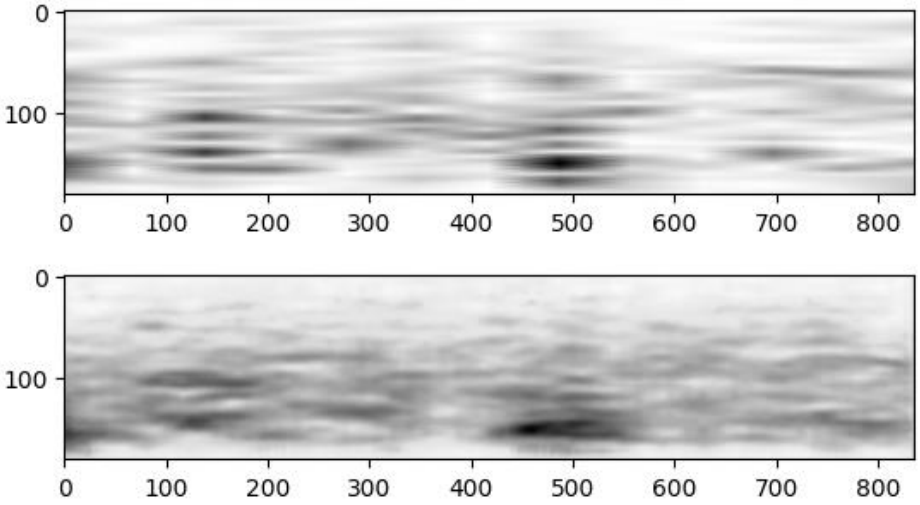

Fig. 8. Comparisons of spectrogram input data and recovered spectrogram input of the autoencoder model with 1D latent space

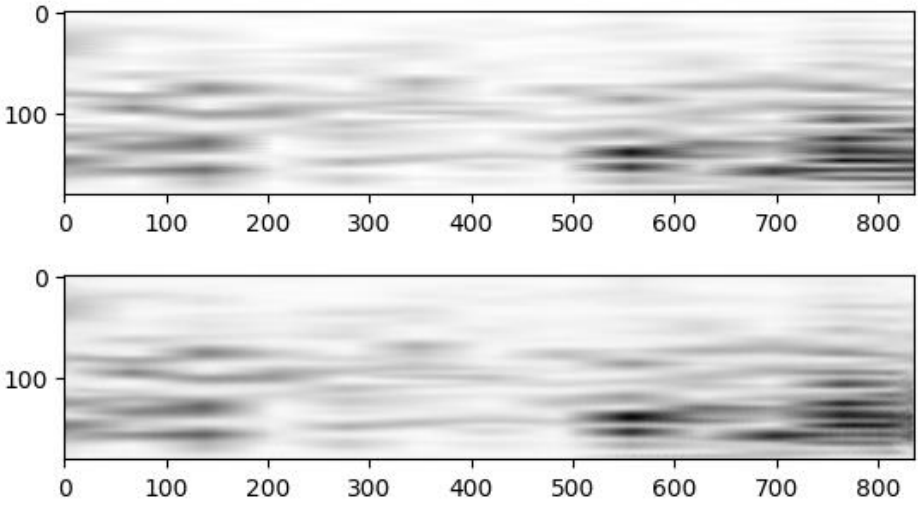

Fig. 9. Comparisons of spectrogram input data and recovered spectrogram input of the autoencoder model with 3D latent space (32x10x51)

Optimization sensitivity is crucial for enhancing the stability and convergence of deep learning models. In this study, we selected the Adam optimizer due to its proven performance in previous research [58]-[60]. However, we also experimented with various hyperparameters, including different optimizers (SGD and Adam), learning rates, batch sizes, and layer architectures.

The results presented in this paper reflect the configurations that achieved the best performance. The choice of the Adam optimizer, along with the selected learning rate and batch size, was based on extensive experimentation and fine-tuning. This process ensured that our model performed optimally under the tested conditions.

While we reported the best-performing results, a more detailed sensitivity analysis could provide further insights into improving training stability and convergence. In future research, we will explore a comprehensive sensitivity analysis and compare alternative optimizers to enhance the robustness of our model across varying conditions. This approach will help ensure that our model maintains high performance in different scenarios and datasets, further validating its effectiveness in EEG-based lie detection.

4.2. Classifier Model Experiment Results

The classifier model experiments involve comparing the classifier model proposed in this research with two other previously developed classifier models. The first model utilizes Conv2D and Fully Connected Layer in its architecture, while the second model incorporates a fine-tuned ResNet50 [61] as the backbone for the classifier model. These existing models serve as benchmarks for evaluating the performance and effectiveness of the proposed autoencoder model. Prior to being inserted into the classifier model, the control and relevant latent space are concatenated together for all three models.

In the training phase, the classifier model undergoes optimization utilizing the SGD (Stochastic Gradient Descent) [62] optimizer combined with the Binary Cross-Entropy (BCE) loss function [63], [64]. The learning process is carefully regulated by employing a specific learning rate of 1e-4, facilitating fine-grained adjustments and contributing to the model's convergence and performance.

In order to evaluate and compare the performance of the three classifier models, we will present several metrics. These metrics include the confusion matrix, which provides insights into the classification results, the F1 Score, which balances precision and recall, and the Accuracy metric, which determines the overall correctness of the models' predictions. By analyzing these additional performance indicators, we can gain a comprehensive understanding of the classifiers' effectiveness and make more informed decisions regarding their usage.

The confusion matrices for each model can be found in Fig. 10 (a, b, c), providing a detailed breakdown of the classification results. Additionally, a comprehensive comparison of the F1 Score and Accuracy metrics is presented in Table 6, allowing for a quantitative evaluation of each model's performance. The confusion matrices revealed that certain types of misclassifications, such as false positives in specific scenarios, could inform model refinement by focusing on improving feature extraction and classification strategies in those areas. From the given confusion matrix of each model, we can calculate the corresponding F1 score and accuracy values, enabling a more thorough analysis of the classification capabilities of each model.

In discussing the results of our research, we have not overlooked ethical considerations and the potential continuation of this study for real-world implementation. Privacy concerns were a primary focus in our study. Personal data of participants is anonymized and not published, ensuring confidentiality. Control questions were designed to be non-invasive and not related to confidential personal information, while relevant questions were based on predefined scenarios to maintain ethical appropriateness. To address potential biases in detection, we included participants from diverse backgrounds, such as high school students, university students, and employees. Future research will involve a more varied demographic pool to enhance the model's generalizability and minimize biases. Different questioning scenarios and improved algorithms will also be tested to enhance accuracy.

We acknowledge the potential legal and social implications of false positives and negatives in lie detection. This study is a preliminary step towards developing a reliable lie detection tool using deep learning. Real-world applications will require detailed testing and approval from relevant authorities to ensure the tool's accuracy and reliability.

Table 6. F1-Score and accuracy for each classifier model on testing set

N	Model Description	F-1 Score	Accuracy	Recall	Precision
1	Proposed Model	0.7333	71.4%	78.57%	68.75%
2	Model with Conv2D and FC layer	0.5600	60.7%	50.00%	63.64%
3	Model with Fine Tuned ResNet50	0.4545	57.1%	35.71%	62.50%

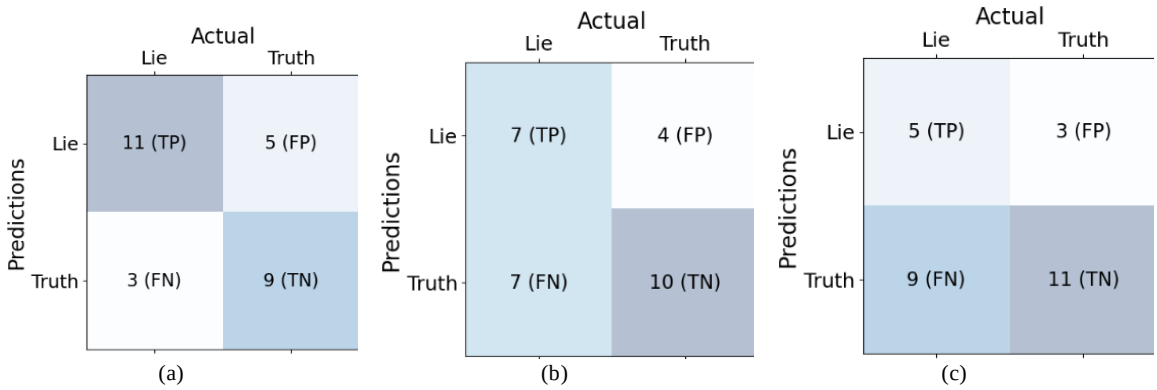

Fig. 10. (a) Confusion matrix of the proposed classifier model, (b) Confusion matrix of the classifier model with conv2d and fully connected layer, (c) Confusion matrix of the classifier model with ResNet50 as the backbone model

Our research is currently in the exploratory phase, focusing on developing an effective deep learning model for lie detection using EEG data. We aim to identify the best deep learning model, utilizing the Muse device for its simplicity, ease of use, and sufficient accuracy, which makes it suitable for real-world applications. Future training will incorporate more diverse demographic data to enhance the model's generalizability. Our current dataset, although collected under controlled conditions, will continue to expand.

Future research will involve testing the models in real-world conditions without predefined scenarios to ensure practical applicability. Although our model is not yet ready for real-world implementation, efforts are ongoing to align it with practical conditions, including real-life trials to refine and validate its performance. Real-world application will also require detailed testing and validation by relevant authorities to ensure the tool's accuracy and reliability.

Future directions include further refining the lie detection tool with multimodal approaches, incorporating sensors for heart rate, respiration, skin conductance, and movement or even video and audio [65]. Continuous improvements in algorithm performance and comprehensive demographic testing will help address ethical concerns. Our goal is to create a more accurate lie detection tool that reduces ethical issues compared to existing technologies like polygraphs [66]. This research is part of a larger effort to improve the accuracy and reliability of lie detection tools, ultimately aiming to mitigate ethical concerns through advanced technology and rigorous testing. We are committed to advancing our model for real-world use, with ongoing improvements and future testing to bridge the gap between controlled experiments and practical applications.

5. Conclusion and Future Work

In this research, we created the lie detection dataset to accomplish the goals of this research, which is lie detection. We developed a dataset that mimics real-life situations by including scenarios related to criminal planning and common questions used in lie detection practice, ensuring realism

without oversimplifying the scenarios or questions. This dataset aims to create a realistic environment and provide a thorough set of questions to effectively assess lie detection techniques.

Additionally, we developed two models capable of effectively detecting whether a person is lying or not based on their EEG data. These models include an autoencoder model and a classifier model, both demonstrating satisfactory performance in lie detection tasks. The autoencoder model effectively reconstructed the input spectrogram images of EEG data, while the classifier model demonstrated proficient classification of truth or lie using the latent space of the EEG spectrogram provided by the autoencoder model with 0.7333 F1-Score and 71.4% Accuracy.

The dataset comprises data from 34 participants aged 16-25, including high school students, undergraduates, and employees, ensuring a degree of demographic diversity. This provides context on its applicability and representativeness. Regarding the provision of a robust dataset, future work will focus on increasing the number of participants, enhancing demographic diversity, and incorporating a variety of real-life scenarios to further improve the model's accuracy and generalizability. Cross-validation ensures model robustness by reducing overfitting. Filtering and normalization mitigate noise in EEG signals, enhancing accuracy. Validation with external datasets, which has not yet been performed, is essential for confirming the model's generalizability in real-world scenarios.

For future work, data preprocessing will utilize wavelet transform, which provides more comprehensive information than STFT, including frequency spectrum with time positioning and multi-scale representation of EEG signals, enabling the detection of features with varying sizes or durations. Wavelet transform is chosen over STFT due to its ability to analyze signals at multiple scales, providing detailed frequency and time information which addresses the limitations of STFT in capturing transient features in EEG data [67], [68]. While this approach presents benefits, we will address potential challenges such as computational complexity, parameter sensitivity, and interpretability of transformed features to ensure its feasibility and practical implementation in EEG-based lie detection.

Additionally, while we currently use attention mechanisms in our classifier, future research will explore their integration in the feature extraction phase to enhance model accuracy. Attention mechanisms can enhance feature extraction by focusing on the most relevant parts of the input data [69], [70], improving model performance as demonstrated in related EEG studies. We acknowledge the trade-offs, such as increased model complexity and overfitting risks, and plan to employ regularization techniques and cross-validation to mitigate these issues, thereby improving the model's robustness and scalability for real-world applications.

Moreover, the selection of EEG channels and frequency bands was based on their physiological relevance to cognitive processes. Channels FP1 and FP2 were chosen for their responsiveness during thinking, and the beta, alpha, and delta frequency bands were selected to capture states of active thinking, relaxation, and deep relaxation, respectively. This approach is grounded in empirical evidence and ensures that the data collected is most relevant for detecting cognitive activities associated with deception. Future work will explore alternative channels and frequency bands, focusing on those correlated with brain functions pertinent to lie detection, to further improve the model's accuracy and applicability.

This study acknowledges the broader implications and ethical considerations associated with EEG-based lie detection technologies. We have taken steps to address privacy concerns, minimize biases, and ensure ethical appropriateness. Future research will focus on expanding demographic diversity, refining algorithms, and ensuring detailed testing and validation by relevant authorities. These steps are crucial to developing a reliable and ethically sound lie detection tool.

This study aims to develop an effective deep learning model for lie detection using EEG data. To enhance generalizability, future research will involve diverse demographic data and real-world testing conditions. Further directions include refining the tool with multimodal approaches and continuous algorithm improvements, ensuring practical applicability and addressing ethical concerns.

Author Contribution: Conceptualization, A.T.H., and Y.K.; methodology, I.A.E., A.P.W., G.N.; software, N.H., Y.K.; validation, G.N., and Y.K.; formal analysis, A.T.H., I.A.E., and A.P.W.; investigation, A.T.H., I.A.E., and A.P.W.; data curation, Y.K.., N.H.; writing—original draft preparation, A.T.H., Y.K., and N.H.; writing—review and editing, A.T.H., Y.K., G.N., and N.H.; visualization, N.H, G.N.; supervision, A.T.H., I.A.E., A.P.W., G.N., Y.K.; funding acquisition, A.T.H., Y.K., N.H. All authors have read and agreed to the published version of the manuscript.

Funding: This work was partially funded by Universitas Negeri Malang under the collaborative research program with Institut Sains dan Teknologi Terpadu Surabaya.

Acknowledgment: The authors would like to thank the managers and the members of the "International Journal of Robotics and Control Systems (IJRCS)" for their precious remarks and suggestions.

Conflicts of Interest: The authors declare no conflict of interest.

References

[1] B. Ranganayakulu, S. M. M, "Brain Fingerprint Technology," *International Research Journal of Modernization in Engineering Technology and Science*, vol. 4, no. 06, pp. 4537-4543, 2022, https://www.irjmets.com/uploadedfiles/paper/issue_6_june_2022/27189/final/fin_irjmets1656499429.pdf.

[2] S. Deepika, B. Kaviyadharshini, S. Sharmila, S. N. Sangeethaa, and S. Jothimani, "A Study on Brain Fingerprinting Technology," *Journal of Ubiquitous Computing and Communication Technologies*, vol. 4, no. 3, pp. 125-137, 2022 https://doi.org/10.36548/jucct.2022.3.001.

[3] A. Farizal, A. D. Wibawa, D. P. Wulandari and Y. Pamungkas, "Investigation of Human Brain Waves (EEG) to Recognize Familiar and Unfamiliar Objects Based on Power Spectral Density Features," *2023 International Seminar on Intelligent Technology and Its Applications (ISITIA)*, pp. 77-82, 2023, https://doi.org/10.1109/ISITIA59021.2023.10221052.

[4] E. P. F. Bareeda, B. S. S. Mohan, and K. V. A. Muneer, "Lie Detection using Speech Processing Techniques," *Journal of Physics: Conference Series*, vol. 1921, no. 1, p. 012028, 2021, https://doi.org/10.1088/1742-6596/1921/1/012028.

[5] A. Pranolo, Y. Mao, A. P. Wibawa, A. B. P. Utama and F. A. Dwiyanto, "Robust LSTM With Tuned-PSO and Bifold-Attention Mechanism for Analyzing Multivariate Time-Series," *IEEE Access*, vol. 10, pp. 78423-78434, 2022, https://doi.org/10.1109/ACCESS.2022.3193643.

[6] A. P. Wibawa, A. B. P. Utama, H. Elmunsyah, U. Pujianto, F. A. Dwiyanto, and L. Hernandez, "Time-series analysis with smoothed Convolutional Neural Network," *Journal of Big Data*, vol. 9, no. 1, p. 44, 2022, https://doi.org/10.1186/s40537-022-00599-y.

[7] I. A. E. Zaeni, U. Pujianto, A. R. Taufani, M. Jiono and P. S. T. Muhammad, "Concentration Level Detection Using EEG Signal on Reading Practice Application," *2019 International Conference on Electrical, Electronics and Information Engineering (ICEEIE)*, pp. 354-357, 2019, https://doi.org/10.1109/ICEEIE47180.2019.8981453.

[8] M. Yazid *et al*., "Simple Detection of Epilepsy From EEG Signal Using Local Binary Pattern Transition Histogram," *IEEE Access*, vol. 9, pp. 150252-150267, 2021, https://doi.org/10.1109/ACCESS.2021.3126065.

[9] A. T. Hermawan, I. A. E. Zaeni, A. P. Wibawa, G. Gunawan, W. H. Hendrawan, Y. Kristian, "A multi representation deep learning approach for epileptic seizure detection," *Journal of Robotics and Control*, vol. 5, no. 1, pp. 187-204, 2024, https://doi.org/10.18196/jrc.v5i1.20870.

[10] A. Rochmah, S. Sendari and I. A. E. Zaeni, "Sleepiness Detection For The Driver Using Single Channel EEG With Artificial Neural Network," *2019 International Conference on Advanced Mechatronics, Intelligent Manufacture and Industrial Automation (ICAMIMIA)*, pp. 80-85, 2019, https://doi.org/10.1109/ICAMIMIA47173.2019.9223371.

[11] M. Žabčíková, Z. Koudelkova, and R. Jašek, "Concealed information detection using EEG for lie recognition by ERP P300 in response to visual stimuli: A review," *WSEAS Transactions on Information Science and Applications*, vol. 19, pp. 171-179, 2022, https://publikace.k.utb.cz/handle/10563/1011270?locale-attribute=en.

[12] M. Zabcikova, Z. Koudelkova and R. Jasek, "EEG-based lie detection using ERP P300 in response to known and unknown faces: An overview," *2022 26th International Conference on Circuits, Systems, Communications and Computers (CSCC)*, pp. 11-15, 2022, https://doi.org/10.1109/CSCC55931.2022.00011.

[13] I. J. Mohammed, L. E. George, "A Survey for Lie Detection Methodology Using EEG Signal Processing," *Journal of Al-Qadisiyah for computer science and mathematics*, vol. 14, no. 1, pp. 42-54, 2022, https://doi.org/10.29304/jqcm.2022.14.1.903.

[14] A. I. Simbolon, A. Turnip, J. Hutahaean, Y. Siagian and N. Irawati, "An experiment of lie detection based EEG-P300 classified by SVM algorithm," *2015 International Conference on Automation, Cognitive Science, Optics, Micro Electro-Mechanical System, and Information Technology (ICACOMIT)*, pp. 68-71, 2015, https://doi.org/10.1109/ICACOMIT.2015.7440177.

[15] I. Nwogu, M. Frank, and V. Govindaraju, "An automated process for deceit detection," *Biometric Technology for Human Identification VII*, vol. 7667, pp. 261-270, 2010, https://doi.org/10.1117/12.851407.

[16] N. Baghel, D. Singh, M. K. Dutta, R. Burget and V. Myska, "Truth Identification from EEG Signal by using Convolution neural network: Lie Detection," *2020 43rd International Conference on Telecommunications and Signal Processing (TSP)*, pp. 550-553, 2020, https://doi.org/10.1109/TSP49548.2020.9163497.

[17] P. Nejedly *et al*., "Utilization of temporal autoencoder for semi-supervised intracranial EEG clustering and classification," *Scientific Reports*, vol. 13, no. 1, p. 744, 2023, https://doi.org/10.1038/s41598-023-27978-6.

[18] Q. Li, Y. Liu, Y. Shang, Q. Zhang, and F. Yan, "Deep Sparse Autoencoder and Recursive Neural Network for EEG Emotion Recognition," *Entropy*, vol. 24, no. 9, p. 1187, 2022, https://doi.org/10.3390/e24091187.

[19] P. Sirpal, R. Damseh, K. Peng, D. K. Nguyen, and F. Lesage, "Multimodal Autoencoder Predicts fNIRS Resting State From EEG Signals," *Neuroinformatics*, vol. 20, p. 537-558, 2022, https://doi.org/10.1007/s12021-021-09538-3.

[20] Y. Wang, S. Qiu, D. Li, C. Du, B. -L. Lu and H. He, "Multi-Modal Domain Adaptation Variational Autoencoder for EEG-Based Emotion Recognition," *IEEE/CAA Journal of Automatica Sinica*, vol. 9, no. 9, pp. 1612-1626, 2022, https://doi.org/10.1109/JAS.2022.105515.

[21] X. Li *et al*., "Latent factor decoding of multi-channel EEG for emotion recognition through autoencoder-like neural networks," *Frontiers in Neuroscience*, vol. 14, p. 87, 2020, https://doi.org/10.3389/fnins.2020.00087.

[22] X. Huang *et al*., "A Novel Epilepsy Detection Method Based on Feature Extraction by Deep Autoencoder on EEG Signal," *International Journal of Environmental Research Public Health*, vol. 19, no. 22, p. 15110, 2022, https://doi.org/10.3390/ijerph192215110.

[23] G. H. Khan, N. A. Khan, M. A. Bin Altaf, and Q. Abbasi, "A Shallow Autoencoder Framework for Epileptic Seizure Detection in EEG Signals," *Sensors*, vol. 23, no. 8, p. 4112, 2023, https://doi.org/10.3390/s23084112.

[24] R. Ramos-Aguilar, J. A. Olvera-López, I. Olmos-Pineda, and S. Sánchez-Urrieta, "Feature extraction from EEG spectrograms for epileptic seizure detection," *Pattern Recognition Letters*, vol. 133, pp. 202–209, 2020, https://doi.org/10.1016/j.patrec.2020.03.006.

[25] B. Mandhouj, M. A. Cherni, and M. Sayadi, "An automated classification of EEG signals based on spectrogram and CNN for epilepsy diagnosis," *Analog Integrated Circuits and Signal Processing*, vol. 108, pp. 101-110, 2021, https://doi.org/10.1007/s10470-021-01805-2.

[26] J. G. Proudfoot, R. Boyle, and R. M. Schuetzler, "Man vs. machine: Investigating the effects of adversarial system use on end-user behavior in automated deception detection interviews," *Decision Support Systems*, vol. 85, pp. 23-33, 2016, https://doi.org/10.1016/j.dss.2016.02.008.

[27] M. C. Morris and J. Z. Morris, "The importance of virtue ethics in the IRB," *Research Ethics*, vol. 12, no. 4, pp. 201-216, 2016, https://doi.org/10.1177/1747016116656023.

[28] D. R. Edla, S. Dodia, A. Bablani, and V. Kuppili, "An Efficient Deep Learning Paradigm for Deceit Identification Test on EEG Signals," *ACM Transactions on Management Information Systems*, vol. 12, no. 3, pp. 1-20, 2021, https://doi.org/10.1145/3458791.

[29] S. Niewiadomski, "Filter Handbook A Practical Design Guide," *First. Oxford: Heinemann Newnes*, 1989, https://gctjaipur.wordpress.com/wp-content/uploads/2015/08/filter-handbook-a-practical-design-guide-s-niewiadomski.pdf.

[30] B. Blankertz, R. Tomioka, S. Lemm, M. Kawanabe and K. -r. Muller, "Optimizing Spatial filters for Robust EEG Single-Trial Analysis," *IEEE Signal Processing Magazine*, vol. 25, no. 1, pp. 41-56, 2008, https://doi.org/10.1109/MSP.2008.4408441.

[31] L. J. Gonçales, K. Farias, L. Kupssinskü, and M. Segalotto, "The effects of applying filters on EEG signals for classifying developers' code comprehension," *Journal of Applied Research and Technology*, vol. 19, no. 6, pp. 584-602, 2021, https://doi.org/10.22201/icat.24486736e.2021.19.6.1299.

[32] A. Kawala-Sterniuk *et al*., "Comparison of smoothing filters in analysis of eeg data for the medical diagnostics purposes," *Sensors*, vol. 20, no. 3, p. 807, 2020, https://doi.org/10.3390/s20030807.

[33] J. S. Kumar and P. Bhuvaneswari, "Analysis of Electroencephalography (EEG) Signals and Its Categorization–A Study," *Procedia Engeering*, vol. 38, pp. 2525-2536, 2012, https://doi.org/10.1016/j.proeng.2012.06.298.

[34] A. Zabidi, W. Mansor, Y. K. Lee and C. W. N. F. Che Wan Fadzal, "Short-time Fourier Transform analysis of EEG signal generated during imagined writing," *2012 International Conference on System Engineering and Technology (ICSET)*, pp. 1-4, 2012, https://doi.org/10.1109/ICSEngT.2012.6339284.

[35] P. Peng, Y. Song, L. Yang, and H. Wei, "Seizure prediction in EEG signals using STFT and domain adaptation," *Frontiers in Neuroscience*, vol. 15, p. 825434, 2022, https://doi.org/10.3389/fnins.2021.825434.

[36] B. Boashash, "Time-frequency signal analysis and processing: a comprehensive reference," *Academic press*, 2015, https://www.sciencedirect.com/book/9780123984999/time-frequency-signal-analysis-and-processing#book-description.

[37] H. Henderi, T. Wahyuningsih, E. Rahwanto, "Comparison of Min-Max normalization and Z-Score Normalization in the K-nearest neighbor (kNN) Algorithm to Test the Accuracy of Types of Breast Cancer," *International Journal of Informatics and Information Systems*, vol. 4, no. 1, pp. 13-20, 2021, https://doi.org/10.47738/ijiis.v4i1.73.

[38] I. Aliyu and C. G. Lim, "Selection of optimal wavelet features for epileptic EEG signal classification with LSTM," *Neural Computing and Applications*, vol. 35, pp. 1077-1097, 2023, https://doi.org/10.1007/s00521-020-05666-0.

[39] M. Grobbelaar *et al*., "A Survey on Denoising Techniques of Electroencephalogram Signals Using Wavelet Transform," *Signals*, vol. 3, no. 3, pp. 577-586, 2022, https://doi.org/10.3390/signals3030035.

[40] H. Adeli, Z. Zhou, and N. Dadmehr, "Analysis of EEG records in an epileptic patient using wavelet transform," *Journal of Neuroscience Methods*, vol. 123, no. 1, pp. 69-87, 2003, https://doi.org/10.1016/S0165-0270(02)00340-0.

[41] A. Géron, "Hands-On Machine Learning with Scikit-Learn, Keras, and TensorFlow: Concepts, Tools, and Techniques to Build Intelligent Systems," *O'Reilly Media*, 2019, https://www.oreilly.com/library/view/hands-on-machine-learning/9781492032632/.

[42] D. L. Gunawan and Y. Kristian, "A Novel Approach to Flexible Multi-Resolution Image Compression using Deep Learning Based Autoencoders on Overlapping Image Patch," *Procedia Computer Science*, vol. 227, pp. 346-354, 2023, https://doi.org/10.1016/j.procs.2023.10.533.

[43] M. Tan and Q. Le, "Efficientnet: Rethinking model scaling for convolutional neural networks," *International conference on machine learning*, 2019, https://doi.org/10.48550/arXiv.1905.11946.

[44] M. Tan and Q. V. Le, "Efficientnetv2: Smaller models and faster training," *International conference on machine learning*, 2021, https://doi.org/10.48550/arXiv.2104.00298.

[45] I. N. Alam, I. H. Kartowisastro, and P. Wicaksono, "Transfer Learning Technique with EfficientNet for Facial Expression Recognition System," *Revue d'Intelligence Artificielle*, vol. 36, no. 4, pp. 543-552, 2022, https://doi.org/10.18280/ria.360405.

[46] Y. Kristian, L. Zaman, M. Tenoyo, and A. Jodhinata, "Advancing Guitar Chord Recognition: A Visual Method Based on Deep Convolutional Neural Networks and Deep Transfer Learning," *ECTI-CIT Transactions*, vol. 18, no. 2, pp. 235-249, 2024, https://doi.org/10.37936/ecti-cit.2024182.254624.

[47] K. Goutam, S. Balasubramanian, D. Gera, and R. R. Sarma, "LayerOut: Freezing Layers in Deep Neural Networks," *SN Computer Science*, vol. 1, no. 295, 2020, https://doi.org/10.1007/s42979-020-00312-x.

[48] D. Tan, W. Zhong, X. Peng, Q. Wang and V. Mahalec, "Accurate and Fast Deep Evolutionary Networks Structured Representation Through Activating and Freezing Dense Networks," *IEEE Transactions on Cognitive and Developmental Systems*, vol. 14, no. 1, pp. 102-115, 2022, https://doi.org/10.1109/TCDS.2020.3017100.

[49] M. D. Coster and J. Dambre, "Leveraging Frozen Pretrained Written Language Models for Neural Sign Language Translation," *Information*, vol. 13, no. 5, p. 220, 2022, https://doi.org/10.3390/info13050220.

[50] A. V. Nair, K. M. Kumar and J. Mathew, "An Improved Approach for EEG Signal Classification using Autoencoder," *2018 8th International Symposium on Embedded Computing and System Design (ISED)*, pp. 6-10, 2018, https://doi.org/10.1109/ISED.2018.8704011.

[51] H. Fu, P. Lei, H. Tao, L. Zhao, and J. Yang, "Improved semi-supervised autoencoder for deception detection," *PLoS One*, vol. 14, no. 10, p. e0223361, 2019, https://doi.org/10.1371/journal.pone.0223361.

[52] M. Aslan, M. Baykara, and T. B. Alakus, "LieWaves: dataset for lie detection based on EEG signals and wavelets," *Medical & Biological Engineering & Computing*, vol. 62, pp. 1571-1588, 2024, https://doi.org/10.1007/s11517-024-03021-2.

[53] T. Nagale and A. Khandare, "Comprehensive Review of Lie Detection in Subject Based Deceit Identification," *Intelligent Computing and Networking*, pp. 89-105, 2023, https://doi.org/10.1007/978-981-99-3177-4_7.

[54] A. Horé and D. Ziou, "Image Quality Metrics: PSNR vs. SSIM," *2010 20th International Conference on Pattern Recognition*, pp. 2366-2369, 2010, https://doi.org/10.1109/ICPR.2010.579.

[55] U. Sara, M. Akter, and M. S. Uddin, "Image Quality Assessment through FSIM, SSIM, MSE and PSNR—A Comparative Study," *Journal of Computer and Communications*, vol. 07, no. 03, pp. 8-18, 2019, https://doi.org/10.4236/jcc.2019.73002.

[56] D. R. I. M. Setiadi, "PSNR vs SSIM: imperceptibility quality assessment for image steganography," *Multimedia Tools and Applications*, vol. 80, pp. 8423-8444, 2021, https://doi.org/10.1007/s11042-020-10035-z.

[57] F. H. Raswa *et al*., "Multi-loss Function in Robust Convolutional Autoencoder for Reconstruction Low-quality Fingerprint Image," *2022 Asia-Pacific Signal and Information Processing Association Annual Summit and Conference (APSIPA ASC)*, pp. 428-431, 2022, https://doi.org/10.23919/APSIPAASC55919.2022.9980345.

[58] L. Muflikhah *et al*., "Single nucleotide polymorphism based on hypertension potential risk prediction using LSTM with Adam optimizer," *Indonesian Journal of Electrical Engineering and Computer Science*, vol. 33, no. 2, pp. 1126-1139, 2024, http://doi.org/10.11591/ijeecs.v33.i2.pp1126-1139.

[59] Y. Wang, Z. Xiao, and G. Cao, "A convolutional neural network method based on Adam optimizer with power-exponential learning rate for bearing fault diagnosis," *Journal of Vibroengineering*, vol. 24, no. 4, pp. 666-678, 2022, https://doi.org/10.21595/jve.2022.22271.

[60] A. K. Shahade, K. H. Walse, V. M. Thakare, and M. Atique, "Multi-lingual opinion mining for social media discourses: an approach using deep learning based hybrid fine-tuned smith algorithm with adam optimizer," *International Journal of Information Management Data Insights*, vol. 3, no. 2, p. 100182, 2023, https://doi.org/10.1016/j.jjimei.2023.100182.

[61] S. Dasari, B. Poonguzhali and M. Rayudu, "Transfer Learning Approach for Classification of Diabetic Retinopathy using Fine-Tuned ResNet50 Deep Learning Model," *2023 International Conference on Sustainable Communication Networks and Application (ICSCNA)*, pp. 1361-1367, 2023, https://doi.org/10.1109/ICSCNA58489.2023.10370255.

[62] J. Sun, Y. Yang, G. Xun, and A. Zhang, "Scheduling Hyperparameters to Improve Generalization: From Centralized SGD to Asynchronous SGD," *ACM Transactions on Knowledge Discovery from Data*, vol. 17, no. 2, pp. 1-37, 2023, https://doi.org/10.1145/3544782.

[63] U. Ruby, P. Theerthagiri, J. Jacob, Y. Vamshidar, "Binary cross entropy with deep learning technique for Image classification," *International Journal of Advanced Trends in Computer Science and Engineering*, vol. 9, no. 4, pp. 5393-5397, 2020, https://doi.org/10.30534/ijatcse/2020/175942020.

[64] C. Guo, X. Chen, Y. Chen, and C. Yu, "Multi-Stage Attentive Network for Motion Deblurring via Binary Cross-Entropy Loss," *Entropy*, vol. 24, no. 10, p. 1414, 2022, https://doi.org/10.3390/e24101414.

[65] K. Mohan and A. Seal, "Deception Detection on 'Bag-of-Lies': Integration of Multi-modal Data Using Machine Learning Algorithms," *Proceedings of International Conference on Machine Intelligence and Data Science Applications*, pp. 445-456, 2021, https://doi.org/10.1007/978-981-33-4087-9_38.

[66] D. Rad, N. Paraschiv, and C. Kiss, "Neural Network Applications in Polygraph Scoring—A Scoping Review," *Information*, vol. 14, no. 10, p. 564, 2023, https://doi.org/10.3390/info14100564.

[67] H. Shayeste and B. M. Asl, "Automatic seizure detection based on Gray Level Co-occurrence Matrix of STFT imaged-EEG," *Biomedical Signal Processing and Control*, vol. 79, p. 104109, 2022, https://doi.org/10.1016/j.bspc.2022.104109.

[68] Ł. Furman, W. Duch, L. Minati, and K. Tołpa, "Short-time Fourier transform and embedding method for recurrence quantification analysis of EEG time series," *European Physical Journal: Special Topics*, vol. 232, pp. 135-149, 2023, https://doi.org/10.1140/epjs/s11734-022-00683-7.

[69] X. Li *et al*., "Deep Learning Attention Mechanism in Medical Image Analysis: Basics and Beyonds," *International Journal of Network Dynamics and Intelligence*, vol. 2, no. 1, pp. 93-116, 2023, https://doi.org/10.53941/ijndi0201006.

[70] Z. Niu, G. Zhong, and H. Yu, "A review on the attention mechanism of deep learning," *Neurocomputing*, vol. 452, pp. 48-62, 2021, https://doi.org/10.1016/j.neucom.2021.03.091.